Supporting Information

"Inferring infection hazard in wildlife populations by linking data across individual and population scales"

Kim M. Pepin, Shannon L. Kay, Ben D. Golas, Susan S. Shriner, Amy T. Gilbert, Ryan S. Miller, Andrea L. Graham, Steven Riley, Paul C. Cross, Michael D. Samuel, Mevin B. Hooten, Jennifer A. Hoeting, James O. Lloyd-Smith, Colleen T. Webb, Michael G. Buhnerkempe

1 Model implementation

We used a Bayesian approach to parameter estimation. All statistical analyses were coded in R programming language (R Core Team, 2015). Priors for the within-host model parameters ($\boldsymbol{\theta}$), were as follows: A $\sim$ Unif$(1, 8)$, $B \sim$ Unif$(1, 30)$, and X_1, X_2, r, and d all had $Gamma(1, 0.1)$ priors. An inverse-gamma prior was used for the variance, σ^2, with shape and scale parameters both equal to 2, and the mean time since infection parameter, λ, had a $Gamma(10, 0.1)$ prior. Posterior distributions were calculated using Markov chain Monte Carlo (50,000 iterations) with a Metropolis-Hastings algorithm on all within-host model parameters ($\boldsymbol{\theta}$), and time since infection in the seroserveillance data ($\boldsymbol{\delta}_2$). A Gibbs sampling algorithm was used for the mean time since infection parameter (λ) as well as the variance parameter on antibody response (σ^2). Convergence was assessed visually with traceplots and the acceptance rates in the Metropolis-Hastings algorithms were between 30-40%. R code for fitting the joint antibody kinetic-serosurveillance model is provided in the Supplementary Information.

2 Simulation to assess model performance

To evaluate performance of the quantitative antibody model, we developed a stochastic population-level disease transmission model that could generate known trajectories of incidence and FOI implemented in Matlab software (Mathworks, R2016b). We used an individual-based model, where individuals were assumed to have an antibody kinetic response upon exposure to infection according to the within-host model described in Eq. 1, which incorporated variability in antibody response curves (i.e., see prior distribution for these parameters above and Tables S1 and S2). Individuals in the population were susceptible, exposed (infected but not infectious), infectious or recovered, and had antibody levels corresponding to the infection curve that began with a lag following exposure (Figure 2). When individuals became infected, they transitioned to infectious after a fixed period of time (1 day) and remained infectious for a period of time that was chosen at random from a Poisson distribution with a mean rate of 7 days (to mimic infection dynamics similar to avian influenza A). Antibody levels were followed in each individual that became infected for the remainder of their life. We assumed a constant population size of 2000 and no seasonality in demographic turnover. The average lifespan of individuals in our simulation was 2 years (lifespan $\sim$ Exp(2)). The population mixed homogenously, the transmission rate was 0.001 per individual per day ($R_0 = 3.8$), and transmission was frequency-dependent. Infection was seeded with a single infectious individual. We recorded the true time of infection for all individuals that became infected. We calculated true incidence as the number of newly infected individuals on day t divided by the total population size at day t. We calculated the true FOI daily using all individuals in the population by dividing the number of newly infected individuals on day t by the total number of susceptible individuals on day $t-1$.

To generate the experimental data (y_1), we simulated antibody quantities every 4 days for one year for each of 30 individuals using the antibody kinetic model (Eq. 1). To generate serosurveillance sampling (y_2) from the population according to a pattern that matched the sampling of snow goose populations (described below), we randomly sampled 200 individuals (10% of the simulated population) each day for one week without replacement. We assumed that the antibody quantification assay did not introduce additional noise. For each individual in the serosurveillance data with antibody concentrations, $y_{2j} > y*$, we estimated the TSI. Using TSI values for all samples and the day on which each sample was collected, we generated a large matrix where rows corresponded to each individual ever sampled, columns were calendar days (t), and values in the matrix were the predicted epidemiological status of each individual on day t (i.e., susceptible, newly infected or seropositive which were back-calculated based on their antibody concentration at the time of sampling). For samples with $y_{2j} \leq y*$, those individuals were added as additional rows in the matrix with a status of susceptible over all time. We derived sample incidence on day t by summing all

newly infected individuals on day t and dividing by the sample size on day t. We derived FOI for day t as the ratio of the number of newly infected individuals in the sample on day t to the number of susceptible individuals in the sample on day $t-1$. Note that this method of deriving FOI assumes homogenous mixing in the population (i.e., all S individuals are available to be infected by infectious individuals at each day t).

3 Parameter Distributions for decay rate simulations

Table 1: Mean and standard deviation of simulated parameter distributions used for the within-host antibody kinetic model (Eq. 1) while varying the decay rate. Parameters: antibody decay rate (d), antibody production rate (r), initial lag between exposure and antibody production (A), period of antibody production in response to infection (B), baseline antibody level prior to exposure (X_1) and increase in baseline antibody levels following antibody decay (X_2). All parameters were simulated from a truncated normal distribution.

	d	r	A	B	X_1	X_2
Fast	0.04 (0.01)	0.11 (0.02)	5 (1.5)	9 (3)	0.082 (0.01)	0.135 (0.01)
Medium	0.01 (0.01)	0.11 (0.02)	5 (1.5)	9 (3)	0.082 (0.01)	0.135 (0.01)
Slow	0.0001 (0.01)	0.11 (0.02)	5 (1.5)	9 (3)	0.082 (0.01)	0.135 (0.01)

4 Systematic Sampling Model

To accommodate systematic serosurveillance sampling, such as sampling individuals weekly or monthly throughout the year (as opposed to just one week out of the year), the model can be adjusted to allow for time-varying mean TSI. Thus, estimates of mean TSI in sampling time unit k (λ_k) are allowed to learn from previous time steps through an auto-regressive process, so that the mean TSI of the samples can vary with epidemiological dynamics according to a normally distributed difference between time steps (η_k). As in the main text, we use a mechanistic model of antibody kinetics, adapted from Simonsen *et al.* (2009), which includes both the rise and decay of antibody levels within hosts (Eq. 1, Fig. 2).

Sampling Serosurveillance Data

Sampling in the serosurveillance data was done without replacement once a week. Approximately 1% of the individuals in the population were randomly sampled on each sampling day (20 individuals each time out of a population of approximately 2000). Thirty individuals were included in each antibody kinetic dataset, with measurements taken on each individual every 4 days for a year (91 observations per individual).

Bayesian Model

Let $\mathbf{y}_{1i}$ denote the antibody kinetic data for individuals $i = 1, ..., n$, and let $y_{2j,k}$ denote the serosurveillance data for individual j sampled on week k. Additionally, let $\delta = k - \tau$ be the time since last infection where τ is the week of the infection and k is the sampling date. Further, assume antibody responses for recently infected individuals are normally distributed around some curve, $g(\boldsymbol{\delta}, \boldsymbol{\theta})$, with curve parameters $\boldsymbol{\theta}$. The model specification is given below where σ^2 is the variance around the curve, $y*$ is a fixed threshold value for indicating whether individual j has been recently infected, and $\delta_{2j,k}$ is the estimated TSI for individual j on sampling week k. The mean TSI for recently infected individuals sampled on week k in the serosurveillance data, λ_k, is autoregressive where λ_0 denotes the TSI infection for the first sampling week in which individuals had titers greater than $y*$. The model specification is then,

$$\mathbf{y}_{1i} = g(\boldsymbol{\delta}_{1i}, \boldsymbol{\theta}) + \epsilon \tag{1}$$

$$y_{2j} = \begin{cases} y_{2j} & y_{2j} \leq y* \\ g(\delta_{2j}, \boldsymbol{\theta}) + \epsilon & y_{2j} > y* \end{cases} \tag{2}$$

$$\epsilon \sim \mathrm{N}(0, \sigma^2) \tag{3}$$

$$X_1 \sim \mathrm{Gamma}(\alpha, \beta) \tag{4}$$

$$X_2 \sim \mathrm{Gamma}(\alpha, \beta) \tag{5}$$

$$r \sim \mathrm{Gamma}(\alpha, \beta) \tag{6}$$

$$d \sim \mathrm{Gamma}(\alpha, \beta) \tag{7}$$

$$A \sim \mathrm{Unif}(0, U_A) \tag{8}$$

$$B \sim \mathrm{Unif}(1, U_B) \tag{9}$$

$$\sigma^2 \sim \mathrm{IG}(r_\sigma, q_\sigma) \tag{10}$$

$$\delta_{2j,k} \sim \mathrm{Pois}(\lambda_k) \tag{11}$$

$$\lambda_k = \lambda_{k-1} + \eta_k \tag{12}$$

$$\eta_k \sim \mathrm{N}(0, \sigma^2_\lambda) \tag{13}$$

$$\lambda_0 \sim \mathrm{Gamma}(\alpha_\lambda, \beta_\lambda) \tag{14}$$

$$\sigma^2_\lambda \sim \mathrm{IG}(r_\lambda, q_\lambda) \tag{15}$$

$$\tag{16}$$

where $\boldsymbol{\theta} = \{X_1, X_2, r, d, A, B\}$, α=1, β=0.1, U_A=8, U_B=30, r_σ and $q_\sigma = 2$, α_λ=10, β_λ=0.1, r_λ=1, and q_λ=1.

Markov Chain Monte Carlo (MCMC) was used to estimate model parameters with 50,000 iterations where a Metropolis-Hastings algorithm was used for all within-host model parameters ($\boldsymbol{\theta}$) as well as $\boldsymbol{\delta}_2$ and η_k, where the acceptance rate was between 30–40%. A Gibbs sampling algorithm was used for the parameters σ_y^2, λ_0, and σ_λ^2. Convergence was assessed visually using traceplots.

The FOI is a derived quantity of the number of newly infected individuals divided by the susceptible individuals in the previous time step. We use a sliding window approach to deriving FOI from systematic serosurveillance sampling to account for long-term changes in individuals' infection status that are not estimable (e.g., how long after or before sampling a susceptible individual should that individual remain classified as susceptible). Therefore, the estimated FOI on week k is calculated based on individuals in the serosurveillance data that were sampled within a sliding window time period, x, which was fixed to be seven weeks in our simulations. Based on each individual's estimated TSI on the week they were sampled, we derive their TSI for every sampling week within the sliding window time period to create a longitudinal dataset of TSI for recently infected individuals. Note in our notation TSI = 0 is the day of infection thus negative values indicate time prior to infection. This longitudinal dataset spans the length of the sliding window period (i.e., seven weeks), where columns correspond to weeks and rows correspond to individuals. Any susceptible individuals (i.e., with $y \leq y^*$) sampled within the sliding window time period are considered susceptibles for the duration of this sliding window time period, and are included in the second term of the denominator in the FOI derivation for all weeks within the sliding window time period (Figure S1). The first term in the denominator for FOI includes seropositive individuals (sampled within the sliding window time period) that are estimated to have a time since infection before week k. Counts of newly infected individuals are also taken from this longitudinal dataset and used in the numerator of the FOI derivation. Thus, point estimates of FOI for week k are averaged since there are multiple point estimates for FOI on each sampling week, with fewer points at the beginning and end of the sampling period (due to the sliding window approach, week k could be included in up to seven different longitudinal datasets described above).

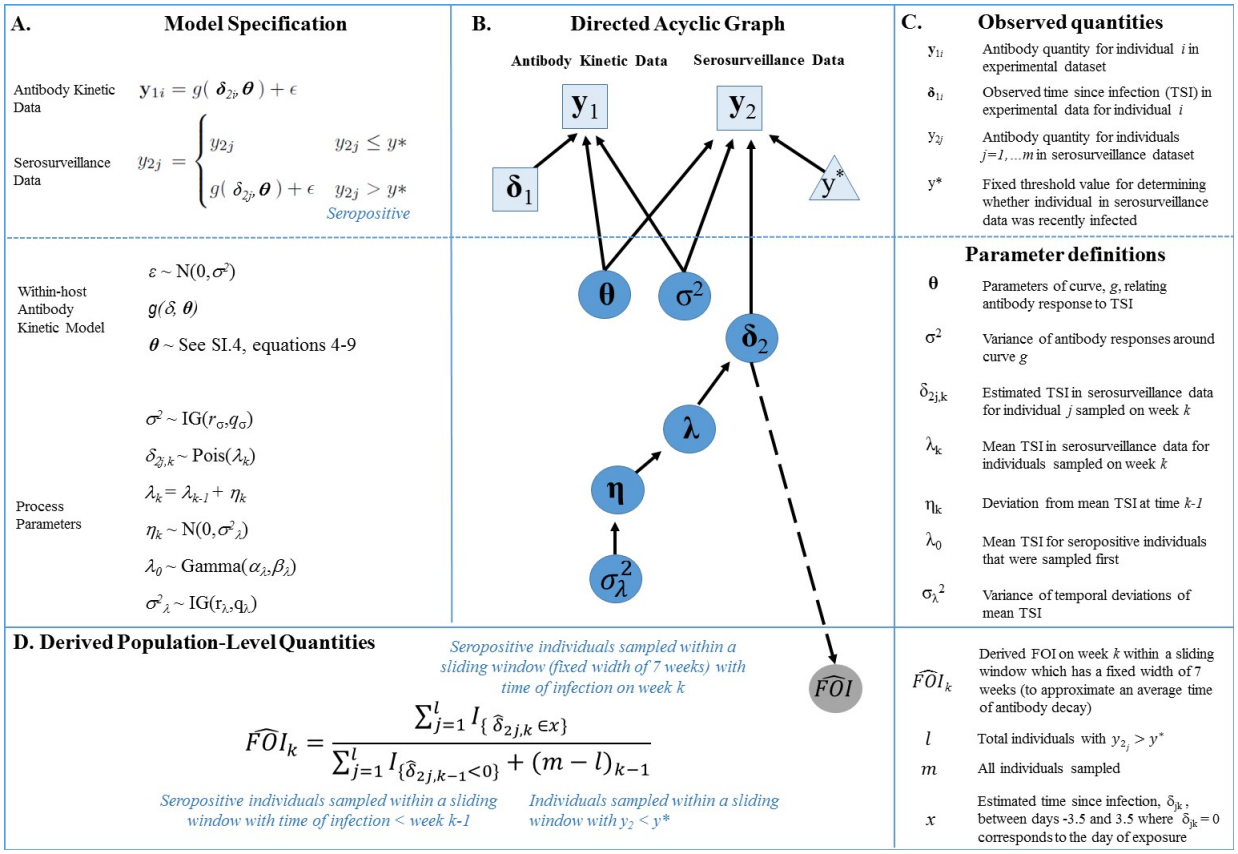

Figure S1: Outline of temporal TSI model. Leftmost column contains model specification, middle panel depicts directed acyclic graph (DAG), and rightmost panel describes observed data and parameters. The bottom panel shows the derivation of FOI.

5 Case study: influenza A in wild birds

Serosurveillance in snow geese. We captured molting, flightless lesser snow geese during July and August on Wrangel Island, Russia during 1993-1995. Geese were banded with U.S. Fish and Wildlife Service metal legbands and most of the adult geese were marked with colored plastic neckcollars engraved with a unique two or three-character code (Samuel et al. 2015) for further details on field methods and AIV diagnostics). We obtained blood samples (< 5 ml) from adult lesser snow geese by jugular venipuncture (Samuel *et al.* 1999). Serum collection and other banding procedures were approved by the U.S. Geological Survey, National Wildlife Health Center, Animal Care and Use Committee. Snow goose sera were tested for antibodies to AIV (regardless of subtype) using the IDEXX FlockChek MultiS-Screen blocking enzyme linked immunosorbent assay (bELISA) according to the manufacturers instructions (IDEXX Laboratories, Westbrook, ME, USA).

Antibody kinetic data in mallards and snow geese. We orally inoculated 10 mallards with 1mL 103 Egg Infectious Dose 50/mL low pathogenic influenza A virus, A/wild bird/IL/183983-24/06(H6N2). Each inoculated bird was co-housed with 3 naive contact birds, all of which became infected by contact with inoculated birds. For all 40 (10 + 3x10) mallards, we collected serum samples from each mallard on days 0, 7, 10, 14, 21, and 28 post inoculation and then every 4-8 weeks for a year. Animal procedures were approved by the U.S.D.A National Wildlife Research Center, Animal Care and Use Committee. Samples were tested for anti-influenza A virus antibodies via the FlockCheck Avian Influenza MultiS-Screen Antibody Test Kit (IDEXX Laboratories, Inc., Westbrook, ME) following the manufacturers instructions except that an alternative threshold of 0.7 was applied and quantitative antibody concentrations were recorded (Shriner *et al.* 2016). On day 380 post inoculation, the ducks were rechallenged with the same virus, again at 10^3 Egg Infectious Dose_{50}/mL and serum samples were collected on days 4, 7, 10, 14, 28 and then every 4 weeks for a second year. Six snow geese were inoculated similarly except they were orally inoculated with one mL 105 Egg Infectious Dose_{50} (EID_{50})/mL of A/mallard/CO/P66F1-5/08 [H4N6] low pathogenic influenza A virus. We collected serum samples on days 2, 4, 7, 10 14, 21, 29, 42, 57 days post infection (dpi), and then every 4 weeks through 365 dpi.

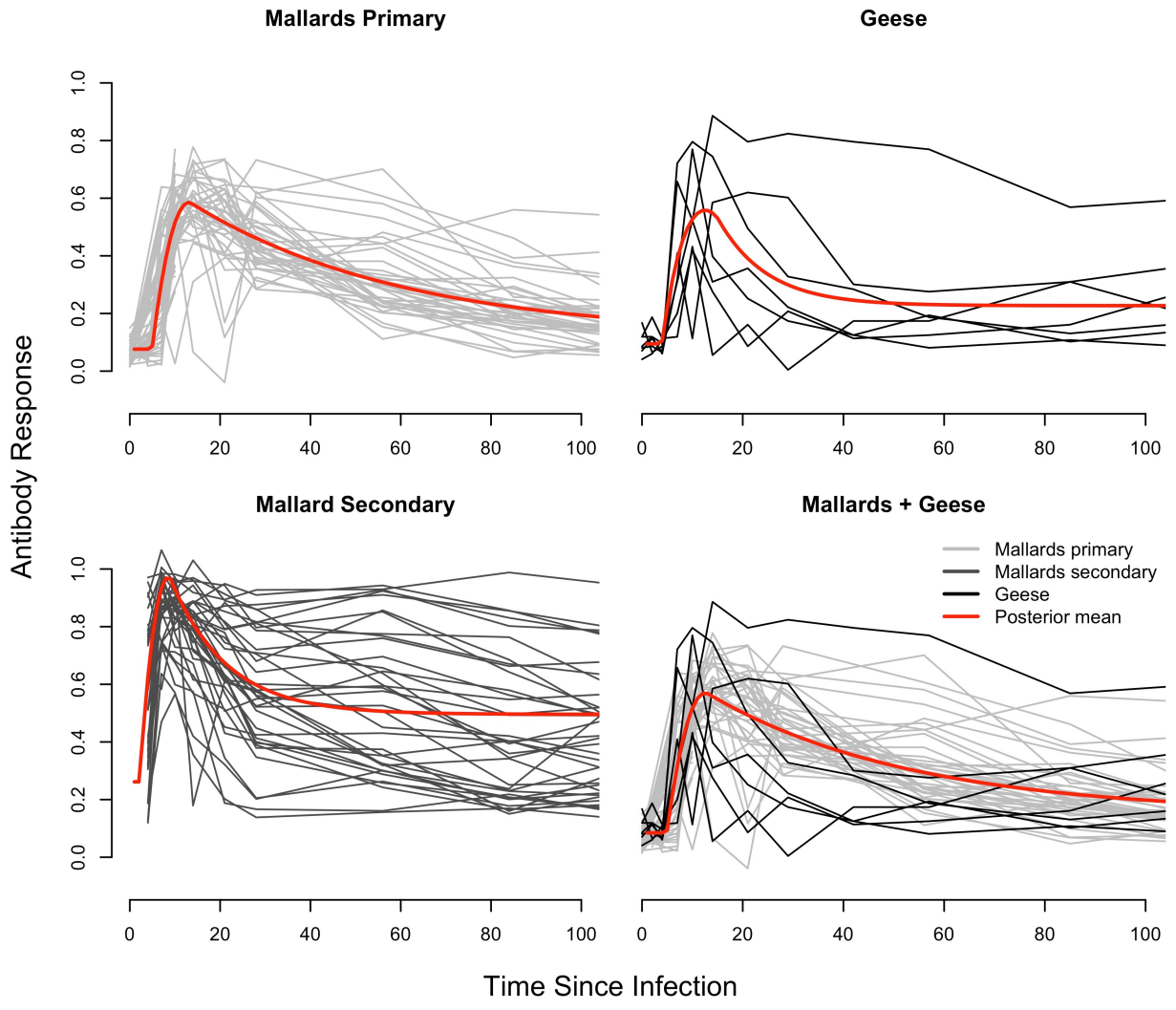

Figure S2: Comparison of antibody kinetics in mallards and snow geese separately (top) and together (bottom right). For the mallards, a secondary inoculation occurred 1 year after the first. The secondary response is shown in the bottom left panel. Red lines indicate predictions from the fitted within-host model (main text Equation 1) to the data shown in each plot.

Table 2: Comparison of mallard and snow geese parameter estimates. Mean and 95% credible intervals of parameter estimates from fitting Eq. 1 (main text) to the experimental mallard and snow geese data. Parameter estimates from the last two columns were used for analyses in Figure 7. Parameters: antibody decay rate (d), antibody production rate (r), initial lag between exposure and antibody production (A), period of antibody production in response to infection (B), baseline antibody level prior to exposure ($X1$), increase in baseline antibody levels following antibody decay ($X2$) and variation around antibody response (σ^2).

	Mallard primary	Mallard secondary	Snow geese primary	Mallard + snow geese primary
d	0.021 (0.015,0.032)	0.08 (0.044,0.18)	0.10 (0.012,0.37)	0.025 (0.16,0.037)
r	0.012 (0.088,0.16)	0.21 (0.12,0.54)	0.11 (0.041,0.25)	0.12 (0.092,0.17)
A	4.9 (3.6,5.7)	2.2 (1.1,3.7)	3.9 (1.4,6.1)	4.9 (3.9,5.7)
B	8.5 (6.4,12)	6.6 (1.6,16.8)	11.0 (2.5,27.7)	7.8 (5.5,10.5)
X_1	0.076 (0.046,0.011)	0.26 (0.031,0.46)	0.095 (0.009,0.19)	0.085 (0.054,0.11)
X_2	0.043 (0.002,0.012)	0.23 (0.034,0.47)	0.13 (0.011,0.26)	0.065 (0.005,0.13)
σ^2	0.017 (0.015,0.020)	0.057 (0.05,0.065)	0.051 (0.037,0.069)	0.022 (0.019,0.025)

6 Simulations: individual-level variation in antibody responses

Table 3: Mean and standard deviation of simulated parameter distributions used for the within-host antibody kinetic model (Eq. 1) with different levels of variation. All parameters were simulated from a truncated normal distribution.

	d	r	A	B	X_1	X_2
Low	0.01 (0.0001)	0.11 (0.002)	5 (0.001)	9 (0.001)	0.082 (0.013)	0.135 (0.001)
Medium	0.01 (0.001)	0.11 (0.02)	5 (1.5)	9 (3)	0.082 (0.013)	0.135 (0.01)
High	0.01 (0.05)	0.11 (0.02)	5 (1.5)	9 (3)	0.082 (0.013)	0.135 (0.01)

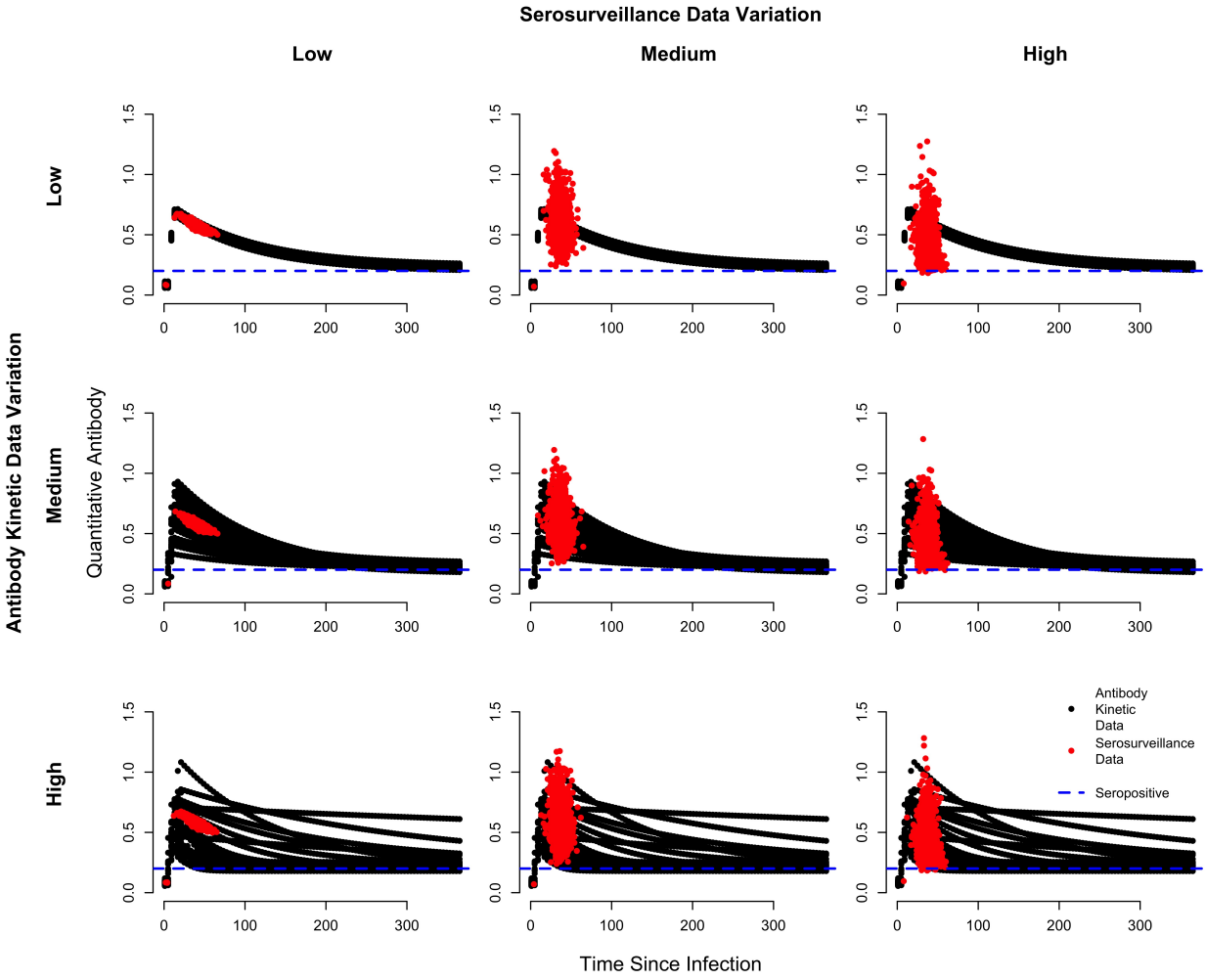

Figure S3: Fits of the model for FOI over time. Predicted FOI with 95% credible intervals is shown in blue with the true FOI plotted in black. Three levels of individual variation were examined: low, medium and high. Rows indicate effects of variation in serosurveillance data while holding variation in antibody kinetic data constant. Columns indicate effects of variation in antibody kinetic data while holding variation in serosurveillance data constant. Table 2 in SI.3 shows the parameter values used for simulating the antibody kinetic and serosurveillance data. Mean values were similar to those estimated from the experimental mallard data. Variances were increased relative to the mallard data to examine effects of higher individual variation.

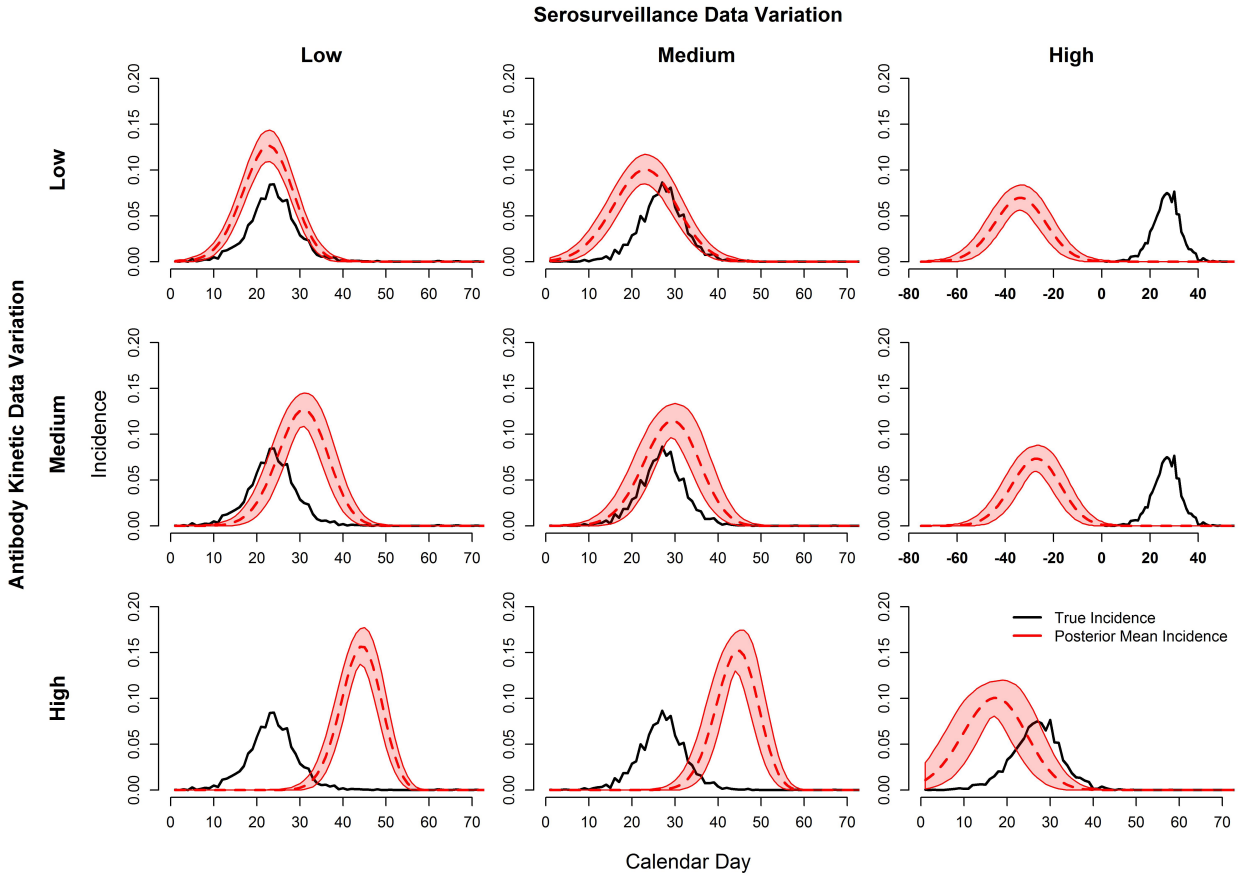

Figure S4: True incidence (black lines) along with posterior mean incidence (red dashed lines) and corresponding 95% credible intervals. Design is similar to Figure S4 and Figure 4 in the main text.

7 Implementation of additional complexities: high variation due to route of exposure variation and anamnestic response

We simulated within-host antibody kinetics using mean values and levels of variation similar to plague in coyotes (Baeten *et al.* 2013) and influenza A in mallards (our data). For plague in coyotes, the intradermal route of exposure leads to much lower antibody levels relative to the oral route of (Baeten *et al.* 2013; Figure S3, top, Table 4), generating high individual-level variation. For influenza A in mallards, the primary infection takes slightly longer to rise and rises and decays more slowly relative to the secondary infection (Figure S2, Table 4, Figure S3, bottom; below). Sixty individuals were included in each antibody kinetic dataset where half of them had oral route of infection or primary antibody responses and the other half had intradermal route of infection or secondary (anamnestic) response. Antibody kinetic measurements were taken on each individual every 4 days for a year (91 observations per individual).

Serosurveillance data were simulated as in SI.2 except that individuals could have antibody responses chosen from one of two distributions (see Table 4 for parameter values). For the route of exposure scenario, oral versus intradermal responses were chosen at random for each individual at the time of infection. For the anamnestic scenario, secondary infections were allowed once antibody titers from primary infection dropped to half the baseline (X_2) value. Secondary infections did not lead to infectiousness, rather they only caused a new antibody response. Sampling of the simulated serosurveillance data was done without replacement once a week. We recorded the route of infection or type of infection (primary versus amannestic) for each infection. Approximately 2.5% of the population was randomly sampled on each sampling day (50 individuals each time out of a population of approximately 2000).

Table 4: Parameter values used to simulate antibody kinetic and serosurveillance data for the route of exposure and anamnestic scenarios. Mean and standard deviation of parameter estimates. These were used for analyses in Figure 8. Antibody kinetics with these parameters are shown in Figure S3. Parameters: antibody decay rate (d), antibody production rate (r), initial lag between exposure and antibody production (A), period of antibody production in response to infection (B), baseline antibody level prior to exposure (X_1), and increase in baseline antibody levels following antibody decay (X_2). Note: coyote d values depended on a threshold r value, where if $r > 0.4$ then mean $d = 0.04$ and if $r \leq 0.4$ then mean $d = 0.02$ (oral); and if $r > 0.12$ then mean $d = 0.08$ and if $r \leq 0.12$ then mean $d = 0.03$ (intradermal).

	Mallard primary	Mallard secondary	Coyote: oral	Coyote: intradermal
d	0.040 (0.01)	0.057 (0.014)	0.02 or 0.04 (0.001)	0.03 or 0.08 (0.001)
r	0.11 (0.02)	0.14 (0.01)	0.35 (0.20)	0.12 (0.05)
A	5 (1.5)	1 (0)	1 (0.5)	1 (0.5)
B	9 (3)	8 (1.1)	14 (0.5)	12 (0.5)
X_1	0.082 (0.01)	0.22 (0.023)	0.01 (0.01)	0.01 (0.05)
X_2	0.14 (0.01)	0.23 (0.028)	1 (0.001)	0.3 (0.01)

A within-host mixture model was added to the Systematic Sampling Model (SI.4 above) to account for

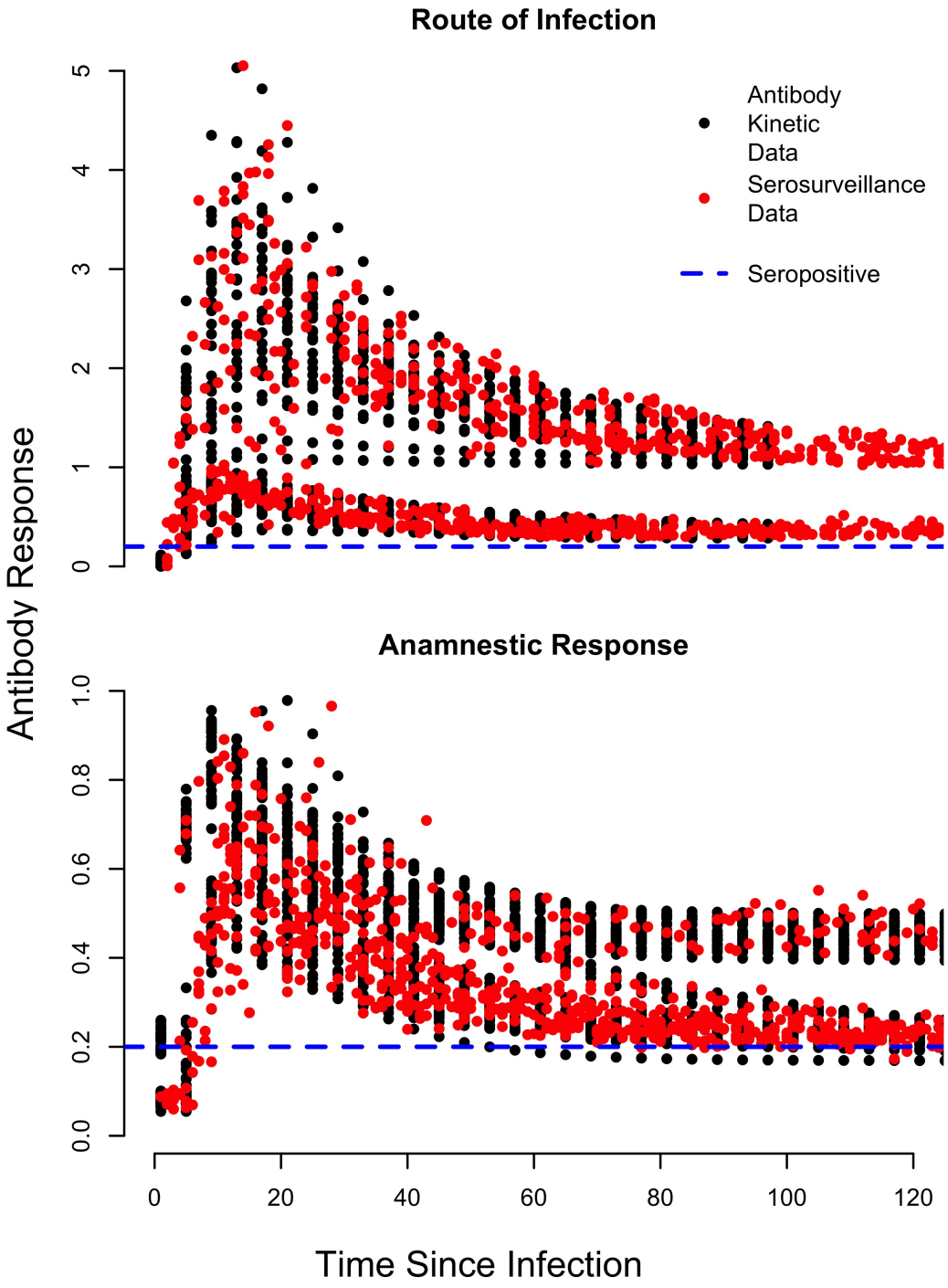

Figure S5: Antibody kinetic data (black) and serosurveillance data (red) which were used in the analyses presented in Figure 8.

differences in types of transmission (i.e., orally vs. intradermally) or infection (i.e., primary vs. secondary), assuming the type of transmission or infection is known. We compared fits of the single-function Systematic Sampling Model to this new mixture model. Let w denote the transmission or infection type, $\boldsymbol{\theta}_1$ denote the parameters of the within-host model $g(\delta, \boldsymbol{\theta})$ for route or response of type 1, and $\boldsymbol{\theta}_2$ denote the parameters for route or response of type 2. Some of the within-host parameters may be shared among the two types, but is not necessary. We assumed global parameters for X_1, A, and B in our simulations, and allowed the parameters r, d, and X_2 to vary by type. Thus, the mean antibody response,

$$g(\delta, \boldsymbol{\theta}) = \begin{cases} g(\delta, \boldsymbol{\theta}_1) & w = 1 \\ g(\delta, \boldsymbol{\theta}_2) & w = 2, \end{cases} \tag{17}$$

is dependent on transmission or infection type (w) as well as time since infection (δ).

MCMC was used to estimate model parameters with 50,000 iterations where a Metropolis-Hastings algorithm was used for all within-host model parameters ($\boldsymbol{\theta}$) as well as $\boldsymbol{\delta}_2$ and η_k, where the acceptance rate was between 30–40%. A Gibbs sampling algorithm was used for the parameters σ_y^2, λ_0, and σ_λ^2. Convergence was assessed visually using traceplots.

8 References

Baeten, L.A., Pappert, R., Young, J., Schriefer, M.E., and Gidleski, T. (2013). Immunological and clinical response of coyotes (*Canis latrans*) to experimental inoculation with *Yersinia pestis*. Journal of Wildlife Diseases, 49, 932-939.

MATLAB and Statistics Toolbox Release 2016b, The MathWorks, Inc., Natick, Massachusetts, United States.

R Development Core Team (2015). R: A language and environment for statistical computing. URL http://www.R-project.org

Samuel, M.D., Shadduck, D.J., Goldberg, D.R., Baranyuk, V., Sileo, L. and Price, J.I. (1999). Antibodies against Pasteurella multocida in snow geese in the western Arctic. Journal of Wildlife Diseases, 35, 440-449.

Samuel, M.D., Hall, J.S., Brown, J.D., Goldberg, D.R., Ip, H. and Baranyuk, V.V. (2015). The dynamics of avian influenza in Lesser Snow Geese: implications for annual and migratory infection patterns. Ecological Applications, 25, 1851-1859.

Shriner, S.A., VanDalen, K.K., Root, J.J. and Sullivan, H.J. (2016). Evaluation and optimization of a commercial blocking ELISA for detecting antibodies to influenza A virus for research and surveillance of mallards. Journal of virological methods, 228, 130-134.